

# Characterization and clinical impact of the tumor microenvironment in post-transplant aggressive B-cell lymphomas

Suvi-Katri Leivonen,<sup>1,2,3</sup> Terhi Friman,<sup>4</sup> Matias Autio,<sup>1,2,3</sup> Samuli Vaittinen,<sup>5</sup> Andreas Wind Jensen,<sup>6</sup> Francesco d'Amore,<sup>6</sup> Stephen Jacques Hamilton-Dutoit,<sup>7</sup> Harald Holte,<sup>8</sup> Klaus Beiske,<sup>9</sup> Panu E. Kovanen,<sup>10</sup> Riikka Rätty<sup>4</sup> and Sirpa Leppä<sup>1,2,3</sup>

<sup>1</sup>Applied Tumor Genomics Research Program, Medical Faculty, University of Helsinki, Helsinki, Finland; <sup>2</sup>Department of Oncology, Helsinki University Hospital Comprehensive Cancer Center, Helsinki, Finland; <sup>3</sup>iCAN Digital Precision Cancer Medicine Flagship, Helsinki, Finland;

<sup>4</sup>Department of Hematology, Helsinki University Hospital Comprehensive Cancer Center and University of Helsinki, Helsinki, Finland; <sup>5</sup>Department of Pathology, Turku University Hospital, University of Turku, Turku, Helsinki, Finland; <sup>6</sup>Department of Hematology, Aarhus University Hospital, Aarhus, Denmark; <sup>7</sup>Institute of Pathology, Aarhus University Hospital, Aarhus, Denmark;

<sup>8</sup>Department of Oncology, Oslo University Hospital, Oslo, Norway; <sup>9</sup>Department of Pathology, Institute for Cancer Research, Oslo University Hospital, Oslo, Norway and <sup>10</sup>Department of Pathology, University of Helsinki, and HUSLAB, Helsinki University Hospital, Helsinki, Finland


**Correspondence:** S. Leppä  
sirpa.leppa@helsinki.fi

**Received:** January 26, 2023.

**Accepted:** May 23, 2023.

**Early view:** June 1, 2023.

<https://doi.org/10.3324/haematol.2023.282831>

Published under a CC BY license 

## Abstract

Post-transplant lymphoproliferative disorders (PTLD) are iatrogenic immune deficiency-associated lymphoid/plasmacytic proliferations developing due to immunosuppression in solid organ or hematopoietic stem cell allograft patients. PTLD are characterized by abnormal proliferation of lymphoid cells and have a heterogeneous clinical behavior. We profiled expression of >700 tumor microenvironment (TME)-related genes in 75 post-transplant aggressive B-cell lymphomas (PT-ABCL). Epstein-Barr virus (EBV)-positive PT-ABCL clustered together and were enriched for type I interferon pathway and antiviral-response genes. Additionally, a cytotoxicity gene signature associated with EBV-positivity and favorable overall survival (OS) (hazard ratio =0.61;  $P=0.019$ ). *In silico* immunophenotyping revealed two subgroups with distinct immune cell compositions. The inflamed subgroup with higher proportions of immune cells had better outcome compared to non-inflamed subgroup (median OS >200.0 vs. 15.2 months;  $P=0.006$ ). In multivariable analysis with EBV status, International Prognostic Index, and rituximab-containing treatment, inflamed TME remained as an independent predictor for favorable outcome. We also compared TME between post-transplant and immunocompetent host diffuse large B-cell lymphomas ( $n=75$ ) and discovered that the proportions of T cells were lower in PT-diffuse large B-cell lymphomas. In conclusion, we provide a comprehensive phenotypic characterization of PT-ABCL, highlighting the importance of immune cell composition of TME in determining the clinical behavior and prognosis of PT-ABCL.

## Introduction

Post-transplant lymphoproliferative disorder (PTLD) is a rare complication and a leading cause of cancer-related mortality following solid organ or allogeneic hematopoietic stem cell transplantation.<sup>1</sup> PTLD are characterized by abnormal proliferation of lymphoid cells associated with immunosuppression and are classified in distinct histological categories (non-destructive, polymorphic, monomorphic) with heterogeneous clinical behavior.<sup>2-4</sup> The majority of monomorphic PTLD are aggressive B-cell lymphomas. The treatment of PTLD depends on the histological type and may include reduction of immunosuppressive therapy, usually combined with immunotherapy and chemotherapy.<sup>5,6</sup>

A substantial proportion (60–80%) of PTLD are associated with Epstein-Barr virus (EBV) positivity.<sup>7,8</sup> As a result of immunosuppression, EBV can promote B-cell proliferation, and potentially transformation, in an unregulated fashion. Typically, EBV-positive PTLD arising in the setting of immunosuppression are associated with a latency type III viral gene expression program and express a wide range of EBV genes, including Epstein-Barr nuclear antigens (EBNA), EBV-encoded small RNA (EBER), and latent membrane proteins (LMP).<sup>5</sup> In contrast, the pathogenesis of EBV-negative PTLD is less understood, and EBV-negative PTLD are considered to resemble lymphomas arising in immunocompetent hosts. EBV-positive and EBV-negative PTLD have been shown to have distinct gene expression

profiles. EBV-positive PTLD is characterized by upregulation of antiviral immune response signaling and markers for immunotolerogenic microenvironment, such as programmed cell death receptor 1 ligand (PD-L1), indoleamine 2,3-dioxygenase 1 (IDO1), and M2-like macrophage marker CD163.<sup>9,10</sup>

The composition and function of the tumor microenvironment (TME) has been shown to have a major impact on development and prognosis of non-immunosuppression-associated lymphomas.<sup>11</sup> Data on the TME in PTLD are more limited, not least because of the rarity of the disease. In addition to the EBV-induced changes in the immune response, the TME in PTLD is markedly affected by the immunosuppressive therapy, which results in an impairment of T-cell immunity. The graft organ also causes chronic immune stimulation through chronic antigen presentation, and prolonged graft-mediated interaction between donor-derived host cells.<sup>12</sup>

In this study, we profiled the expression of over 700 TME-related genes in 75 monomorphic post-transplant aggressive B-cell lymphomas (PT-ABCL) and correlated the findings with patient demographics and outcome. In addition, we compared the TME of post-transplant diffuse large B-cell lymphomas (PT-DLBCL) with that found in sporadic DLBCL. Our data support previous studies that have found differences between EBV-positive and EBV-negative PT-ABCL and provide evidence of a favorable impact of the T-cell-inflamed TME on the survival of patients with PT-ABCL.

## Methods

### Patients and samples

The study cohort included 75 patients with PT-ABCL diagnosed between 1997 and 2021 at the Helsinki (Finland), Turku (Finland), Oslo (Norway) and Aarhus (Denmark) University Hospitals (Table 1). All patients had received solid organ transplants and were >16 years old at the time of PTLD diagnosis. The histopathological diagnoses of all cases were reviewed and confirmed by expert hematopathologists and classified according to the World Health Organization classification of the lymphoid neoplasms (2016 revision).<sup>4</sup> All study cases met the morphological and immunophenotypic criteria for the diagnosis of monomorphic PTLD. In particular, cases of non-destructive PTLD and polymorphic PTLD were excluded. Further details of the patients and their treatment are provided in the *Online Supplementary Appendix*. The study protocol, including biobanking, was approved in Finland by Helsinki Biobank permission (HUS/190/2018), the Ethics Committee of the Helsinki University Hospital (194/13/03/00/16 and 1916/2018§108), and by the National Institution for Health and Welfare (THL/1001/5.05.00/2016), in Norway by the Regional Committee for Medical and Health Research Ethics South-East

(191426) and in Denmark by the Aarhus University Hospital Ethics Committee (M-2021-45-21).

The cohort of immunocompetent host DLBCL included 75 samples from patients with sporadic high-risk DLBCL not-otherwise-specified (NOS) treated in the Nordic LBC-05 and LBC-04 trials with biweekly R-CHOEP (ri-

**Table 1.** The Nordic post-transplant aggressive B-cell lymphoma cohort.

Characteristics	N (%)
Patients	75 (100)
Sex	
Female	27 (36)
Male	48 (64)
Age in years at PTLD diagnosis, median (range)	56 (16-76)
<60	47 (63)
≥60	28 (37)
Histology	
DLBCL, NOS	59 (79)
GCB	15 (26)
Non-GCB	19 (32)
NA	25 (42)
PCNSL	9 (12)
Burkitt	6 (8)
HGBL-triple hit	1 (1)
Stage	
Early (1-2)	30 (40)
Advanced (3-4)	36 (48)
NA	9 (12)
IPI	
Low (0-2)	32 (43)
High (3-5)	34 (45)
NA	9 (12)
EBER	
Positive	42 (56)
Negative	26 (35)
NA	7 (9)
Time from transplantation to PTLD in years, median (range)	9 (0.1-34)
<1	14 (19)
1-5	16 (21)
>5	45 (60)
Transplant	
Kidney	36 (48)
Liver	8 (12)
Heart	16 (22)
Lung	10 (13)
Kidney + Pancreas	3 (4)
Lung + Heart	1 (1)
NA	1 (1)
Rituximab-containing treatment	
Yes	53 (71)
No	21 (28)
NA	1 (1)

PTLD: post-transplant lymphoproliferative disorder; DLBCL, NOS: diffuse large B-cell lymphoma, not otherwise specified; GCB: germinal center B cell; PCNSL: primary central nervous system lymphoma; HGBL: high-grade B-cell lymphoma; NA: not assigned; IPI: International Prognostic Index; EBER: Epstein-Barr virus-encoded small RNA.

tuximab, cyclophosphamide, doxorubicin, etoposide and prednisone) immunochemotherapy and systemic central nervous system (CNS) prophylaxis (high-dose methotrexate and cytarabine).<sup>13,14</sup> The gene expression profiling results for these DLBCL patients have been previously described.<sup>15</sup>

### Gene expression profiling

RNA isolation and gene expression profiling are described in detail in the *Online Supplementary Appendix*. Briefly, RNA was extracted from formalin-fixed paraffin-embedded (FFPE) lymphoma blocks and subjected to gene expression analysis utilizing the Nanostring nCounter platform with the Human PanCancer Immunoprofiling Panel codeset (XT-CSO-HIP1-12, NanoString Technologies, Seattle, WA).

### Immune cell phenotyping

For *in silico* immune cell phenotyping, we applied the CIBERSORTx algorithm,<sup>16,17</sup> which uses a set of reference gene expression values (an LM22 signature matrix of 547 genes) to infer the cell type proportions from gene expression data. In order to run CIBERSORTx, normalized gene expression data were uploaded to the CIBERSORTx web portal (<http://cibersortx.stanford.edu/>) and the algorithm run using the default LM22 signature matrix at 100 permutations.

Details on the multiplex immunohistochemistry (mIHC) stainings are provided in the *Online Supplementary Appendix*.

### Statistical analysis

All data analysis was performed using R version 4.0.2. Un-

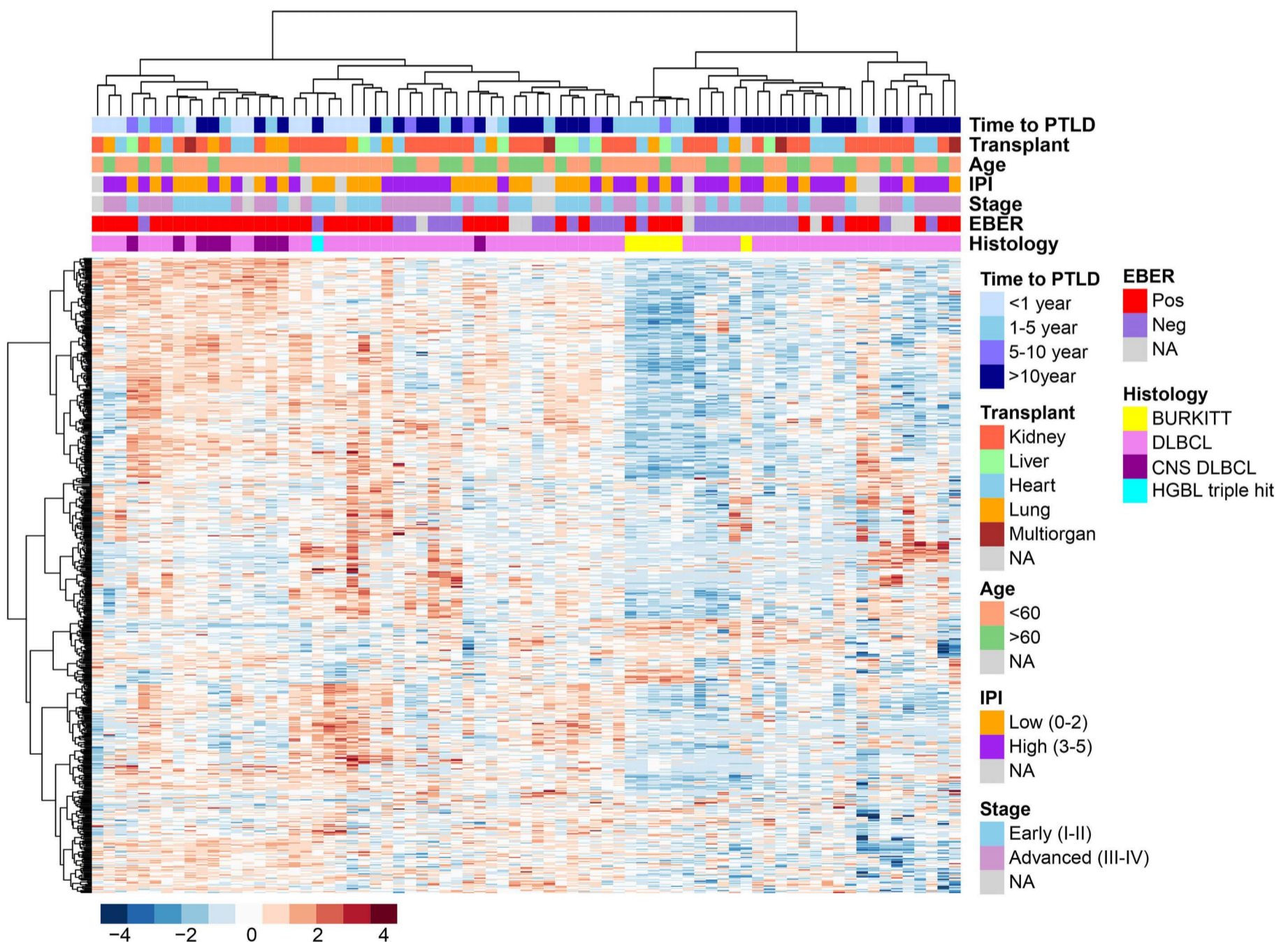


**Figure 1. Unsupervised clustering of post-transplant aggressive B-cell lymphoma samples.** The heatmap visualizes unsupervised hierarchical clustering of the immune panel gene expression data from 75 post-transplant aggressive B-cell lymphoma (PT-ABCL) samples. Z-score transformed levels of gene expression are depicted according to the color scale shown. Rows represent genes and columns represent samples from PT-ABCL patients. NA: not assigned; IPI: International Prognostic Index; EBER: Epstein-Barr virus-encoded small RNA; pos: positive; neg: negative; HGBL: high-grade B-cell lymphoma; DLBCL: diffuse large B-cell lymphoma; CNS: central nervous system.

supervised clustering with Euclidean distance and ward. D linkage was carried out by the “pheatmap” package. The R package “limma” was utilized for differential gene expression analysis, whereas Wilcoxon rank sum test and Kruskal-Wallis tests were used for non-parametric comparisons between two or more groups, respectively. The Fisher’s exact test was used to assess whether differences in dichotomous clinical variables were significant between groups. *P* values were corrected for multiple testing using the Benjamin-Hochberg method. For survival analysis, Kaplan-Meier estimates with log-rank test, as well as Cox univariable and multivariable regression analysis were used.

## Results

### Baseline characteristics and patients outcome

Baseline characteristics of the PT-ABCL patients (n=75) are presented in Table 1. Majority of the cases (n=59, 79%) had DLBCL histology. In addition, there were nine (12%) PCNSL, six (8%) Burkitt lymphomas, and one triple-hit high-grade B-cell lymphoma. In total, 56% of the PT-ABCL were EBV-positive, 35% were EBV-negative, and in 9% the EBV status was unknown. The time from transplantation to PTLD was highly dependent on the EBV status (linear regression  $P=4.86e-05$ ) and all patients with early-onset disease (<1 year from transplantation, n=14, 19%) were EBV-positive. The median time from organ transplant to lymphoma diagnosis was 9.0 years (range, 0.1-34.0), and the median follow-up time was 10.7 years (interquartile range [IQR], 6.0-13.8). The median overall survival (OS) after lymphoma diagnosis was 4.3 years (IQR, 0.3-infinite) and median progression-free survival (PFS) was 2.8 years (IQR, 0.3-infinite).

Younger age (<60 years), low IPI (0-2) and early stage (I-II) were associated with better OS and PFS (*Online Supplementary Figure S1A, B*), whereas the EBV status, type of the transplanted organ, and PTLD histology were not significantly associated with the outcome. Patients with earlier onset of the disease (<5 years) had a better outcome, but the result was not statistically significant (*Online Supplementary Figure S1A, B*).

### Gene expression profile of post-transplant aggressive B-cell lymphomas

Gene expression profiling demonstrated a high degree of heterogeneity and variation in the immune response profile among PT-ABCL (Figure 1). Two major clusters were identified, and majority of the EBV-positive samples (71%, 30/42) clustered together, but the other clinical factors were not segregated into their own groups based on the gene expression. Most of the post-transplant Burkitt lymphomas formed their own subcluster character-

ized by low expression of genes, which typically distinguish Burkitt lymphomas from DLBCL, such as NF- $\kappa$ B target gene and MHC class I signature<sup>18</sup> (*Online Supplementary Figure S2*). On the contrary, post-transplant PCNSL with DLBCL histology shared the gene expression profile with a subset of PT-DLBCL (Figure 1; *Online Supplementary Figure S3*). This is in line with previous reports showing that according to their gene expression profile, PCNSL do not differ markedly from systemic DLBCL with regard to their gene expression profile but are instead distributed within the spectrum of DLBCL.<sup>19</sup> However, since PCNSL are clinically considered to be a distinct entity with poor prognosis,<sup>20</sup> we excluded these cases from further analyzes.

### Differential profiles between Epstein-Barr virus-positive and Epstein-Barr virus-negative post-transplant aggressive B-cell lymphomas

EBV status plays a major role in the development of PTLD.<sup>21</sup> Since unsupervised clustering analysis indicated that EBV-positive and EBV-negative cases have distinct gene expression profiles (Figure 1), we explored the differentially expressed genes based on the EBV status. EBV-negative cases were characterized by expression of the MHC class II genes (*HLA-DMB*, *HLA-DMA*, *HLA-DOB*) as well as B-cell development-associated genes, such as *MS4A1*, *CD79B*, and *SYK*, whereas in EBV-positive cases type I interferon signaling pathway and antiviral response genes, including *IFITM1*, *ISG15*, *MX1*, and *IFI35*, were enriched (Figure 2A, B; *Online Supplementary Table S1*). In addition, genes previously shown to associate with EBV positivity, *IDO1* and granzymes (*GZMB*, *GZMH*, *GZMA*),<sup>9,22</sup> were upregulated in EBV-positive cases.

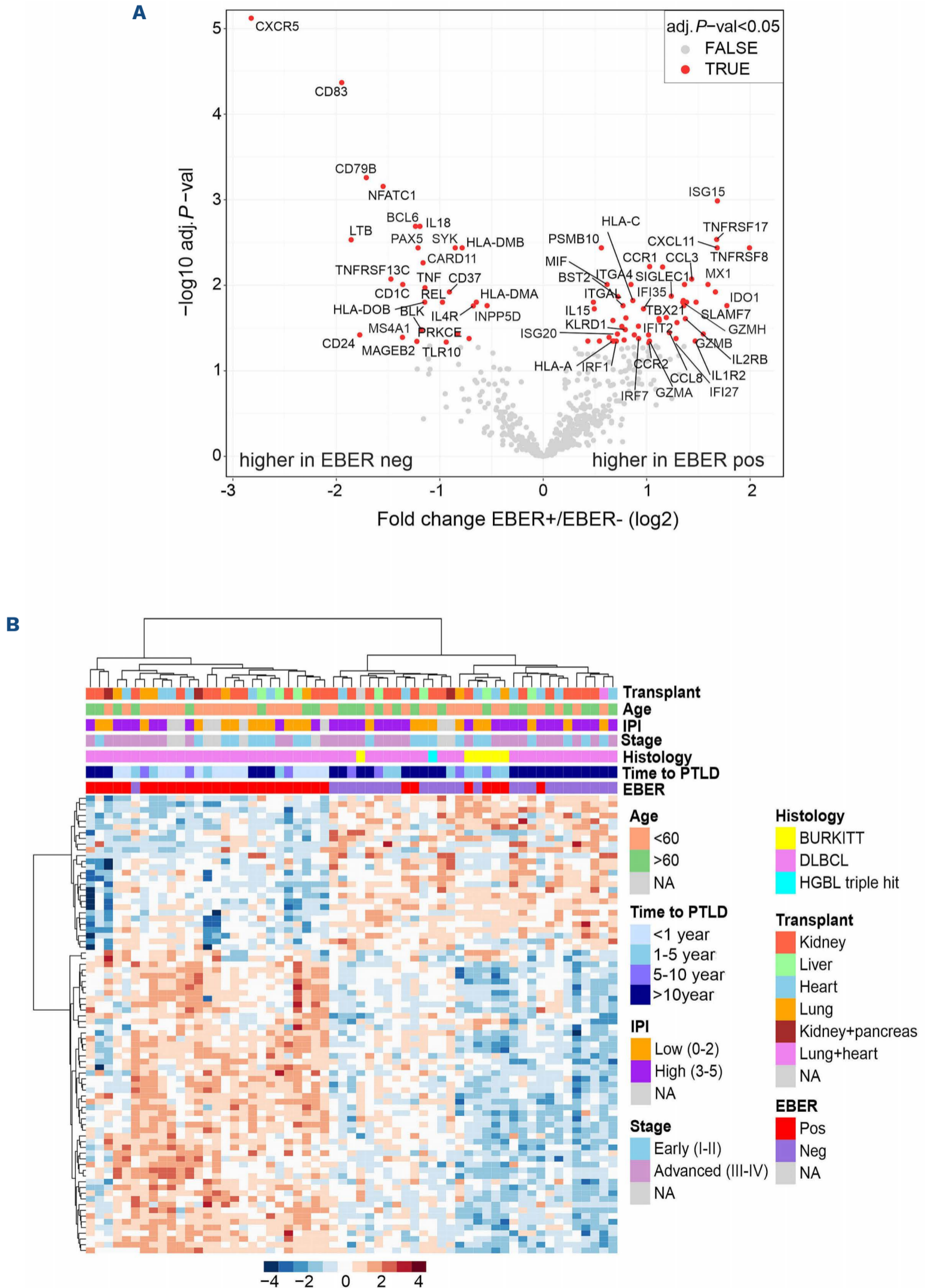
Gene expression-based *in silico* deconvolution of the proportions of distinct immune cells indicated that EBV-negative PT-ABCL had a higher proportion of B cells and follicular T helper ( $T_{FH}$ ) cells, whereas in EBV-positive PT-ABCL proportions of infiltrating T cells, especially memory CD4 T cells, and plasma cells were higher (Figure 2C). No significant differences in the proportions of macrophages were found (*data not shown*).

### Cytotoxicity gene signature predicts better outcome

Next, we focused on specific gene signatures in the Nanostring immune panel and extracted genes for the cytotoxic signature: *HLA-A*, *HLA-B*, *HLA-C*, *GZMA*, *GZMB*, *GZMH*, *GZMK*, *GZMM*, *GZML*, and *PRF1*. Interestingly, we noticed that expression of the cytotoxic signature divided the patients into three distinct groups (Figure 3A), of which the high cytotoxicity group was associated with EBV positivity and earlier onset of the disease (*Online Supplementary Table S2*). The group with the highest cytotoxicity signature expression had significantly better OS compared with the low or intermediate groups (ha-

zard ratio [HR] =0.61; 95% confidence interval [CI]: 0.40-0.92;  $P=0.019$ ) (Figure 3B), suggesting that the inflammation status of the TME plays a role in the prognosis of

PTLD. In contrast, the cytotoxic signature was not associated with outcome in sporadic DLBCL (*Online Supplementary Figure S4*).



Continued on following page.

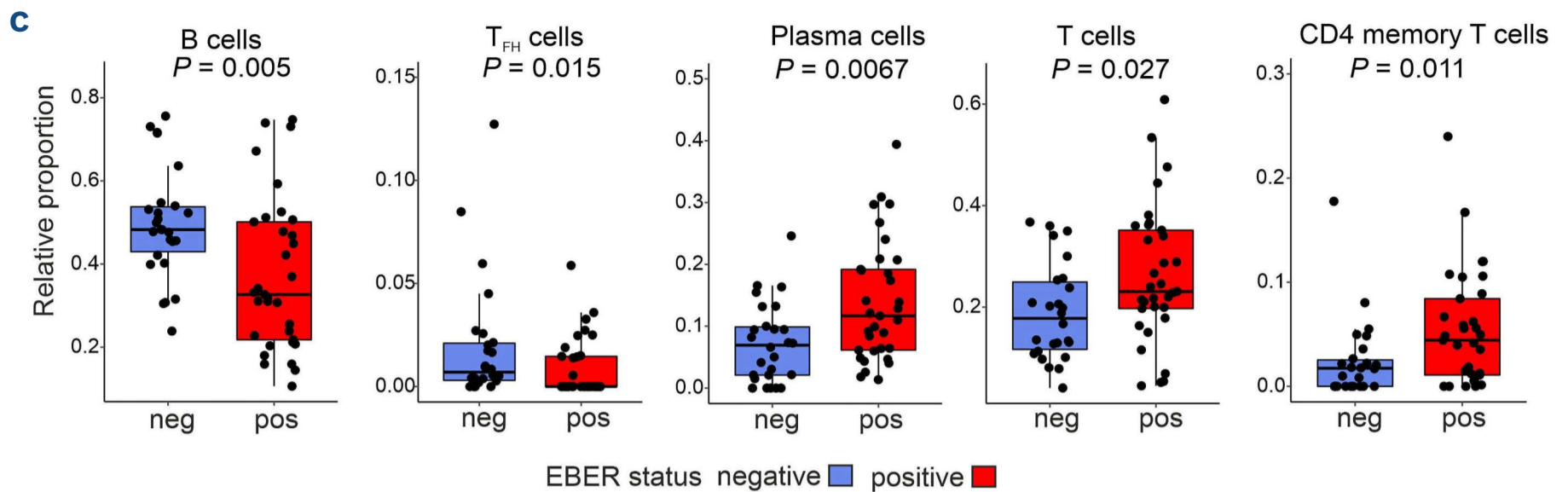


**Figure 2. Differential gene expression based on the Epstein-Barr virus status of post-transplant aggressive B-cell lymphoma.** (A) Volcano plot showing differentially expressed genes by the Epstein-Barr virus (EBV) status. The genes with  $\log_2$  fold change  $>0$  have higher expression in EBV-positive post-transplant aggressive B-cell lymphoma samples (PT-ABCL), whereas the genes with  $\log_2$  fold change  $<0$  have higher expression in EBV-negative PT-ABCL. (B) Unsupervised hierarchical clustering of the differentially expressed genes with adj.  $P < 0.05$ . (C) The proportions of 22 distinct immune cell types were estimated with the CIBERSORTx algorithm. The box-plots show the main cell types with significantly different proportions in EBV-positive vs. EBV-negative PT-ABCL (Mann-Whitney test). NA: not assigned; IPI: International Prognostic Index; EBV: Epstein-Barr virus-encoded small RNA; pos: positive; neg: negative; HGBL: high-grade B-cell lymphoma; DLBCL: diffuse large B-cell lymphoma.

### Post-transplant aggressive B-cell lymphoma patients with T-cell-inflamed tumor microenvironment have better outcome

In order to characterize the immune cell landscape of PT-ABCL in more detail, we performed unsupervised hierarchical clustering with CIBERSORTx deconvoluted immune cell types (Figure 4A). PT-ABCL clustered into two main groups: the smaller group ( $n=23$ , 35%) with inflamed TME was characterized by the presence of T cells, M1- and M2-like macrophages, and NK cells, but low B-cell proportions, whereas the non-inflamed group ( $n=43$ , 65%) had low proportions of T cells, higher macrophage/T-cell ratio, and high proportions of B cells. The inflamed subgroup was also enriched for the cytotoxic gene signature (Figure 4A). *In silico*-estimated cell proportions correlated well with multiplex immunohistochemistry stainings, which were available for a small subset of patients, corroborating the CIBERSORTx data (Figure 4B; *Online Supplementary Figure S5*). The inflamed subgroup was associated with EBV positivity ( $P=0.008$ ) and with earlier onset of PTLD following transplantation ( $P=0.004$ ) (Table 2). The type of transplant organ was not associated with the inflammation status of the TME ( $P=0.206$ ), nor did the main immune cell types differ by the transplant organ (*Online Supplementary Figure S6*). In line with previous studies on DLBCL and other lymphomas,<sup>23-27</sup> inflamed PT-ABCL TME translated to better outcome (median OS  $>200.0$  vs. 15.2 months;  $P=0.006$ ; median PFS 89.0 vs. 14.4 months,  $P=0.049$ ) (Figure 4C; *Online Supplementary Figure S7*). In multivariable analysis with EBV status, IPI and rituximab-containing treatment, the inflamed TME remained as an independent predictor for

favorable OS and PFS (Figure 4D). This highlights the importance of the TME also in PTLD despite the immunosuppressive treatment.

Of the individual immune cells, the presence of resting dendritic cells (OS: HR=2.7; 95% CI: 1.3-5.5;  $P=0.008$ , and PFS: HR=2.5; 95% CI: 1.2-5.2;  $P=0.013$ ) and activated mast cells (OS: HR=5.4; 95% CI: 1.8-16.0;  $P=0.009$ , and PFS: HR=4.8; 95% CI: 1.7-14,  $P=0.004$ ) translated to unfavorable outcome, whereas regulatory T cells were associated with longer survival (OS: HR=0.05; 95% CI: 0.0-0.8;  $P=0.035$ , and PFS: HR=0.1; 95% CI: 0.1-1.0;  $P=0.046$ ) (*Online Supplementary Table S3A, B*). In multivariable analysis with rituximab-containing treatment and IPI, activated mast cells remained as independent predictors for worse, and regulatory T cells (Tregs) for improved, OS and PFS (*Online Supplementary Table S3C*).

### Comparison of post-transplant diffuse large B-cell lymphomas with sporadic diffuse large B-cell lymphomas

We next compared the PT-DLBCL ( $n=59$ ) with DLBCL-NOS of immunocompetent hosts ( $n=75$ ). Regarding clinical characteristics of the two cohorts, the sporadic DLBCL cohort was enriched for high-risk, advanced-stage patients, whereas neither age nor IPI were significantly different between the cohorts (*Online Supplementary Table S4*). Interestingly, principal component analysis and unsupervised clustering of the gene expression data indicated that PT-DLBCL did not form their own subgroup, but rather clustered closely with sporadic DLBCL (Figure 5A; *Online Supplementary Figure*

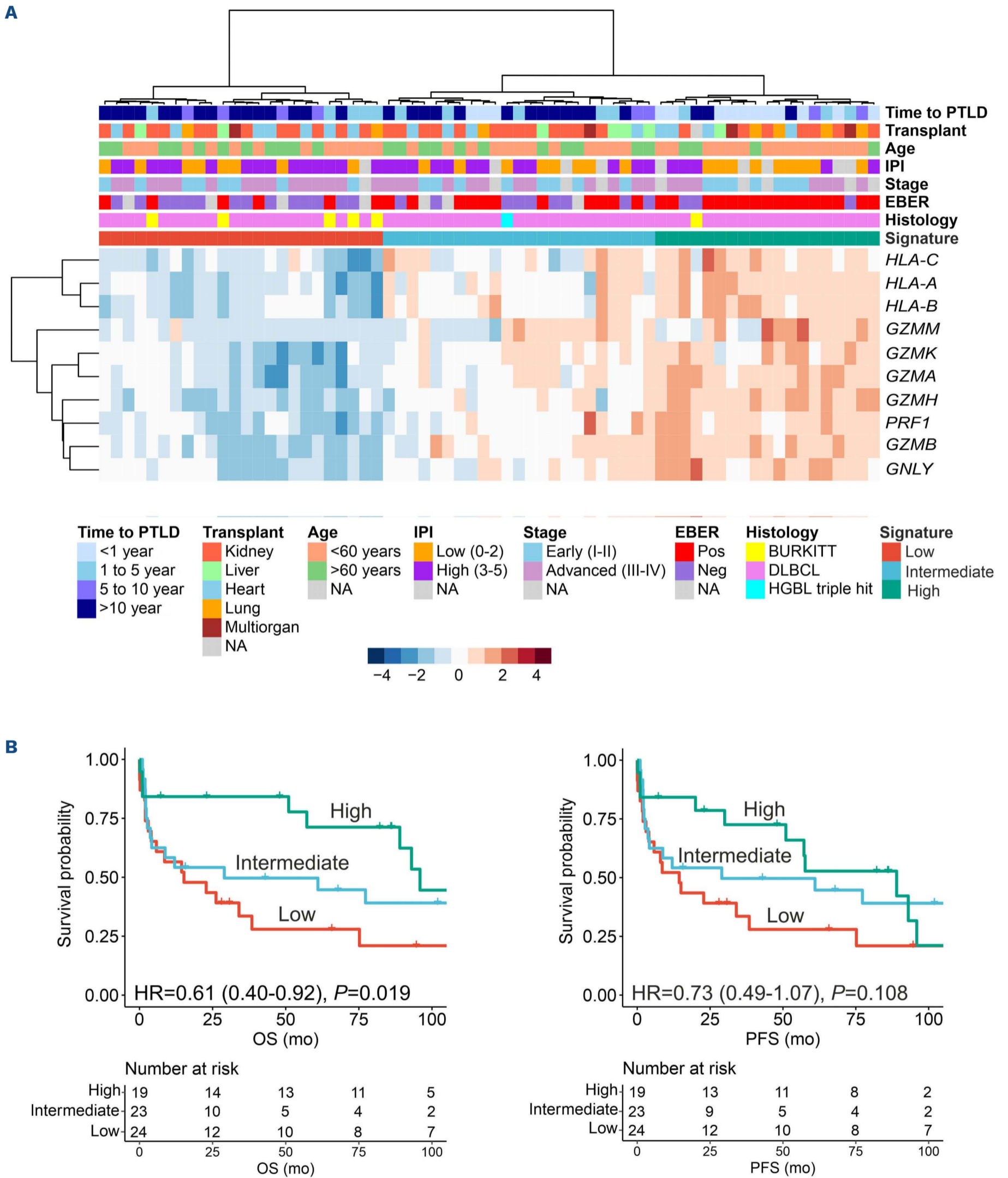
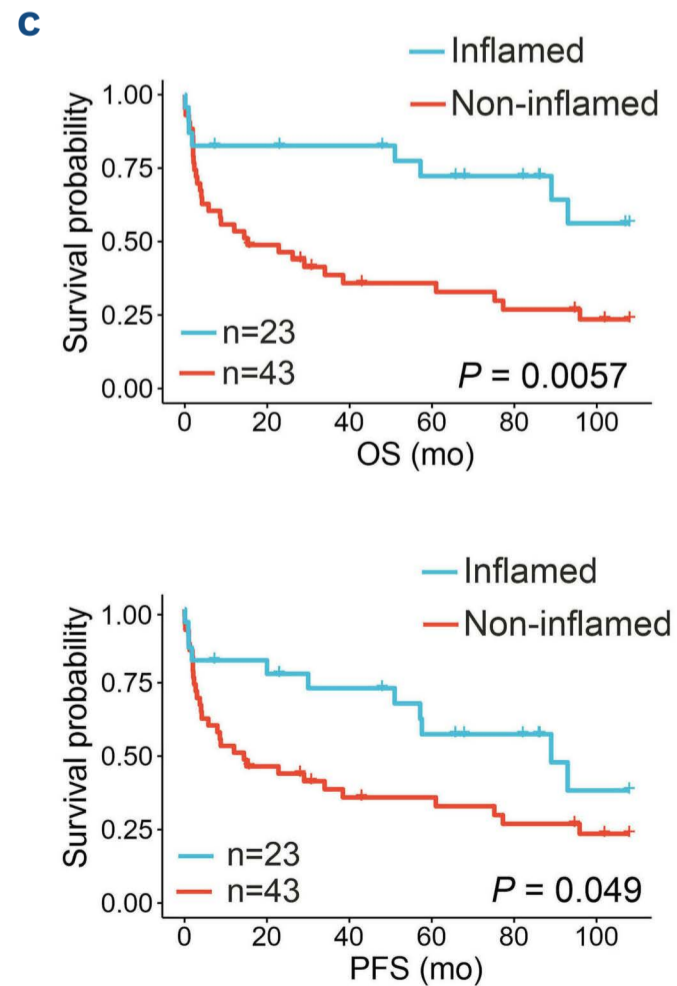
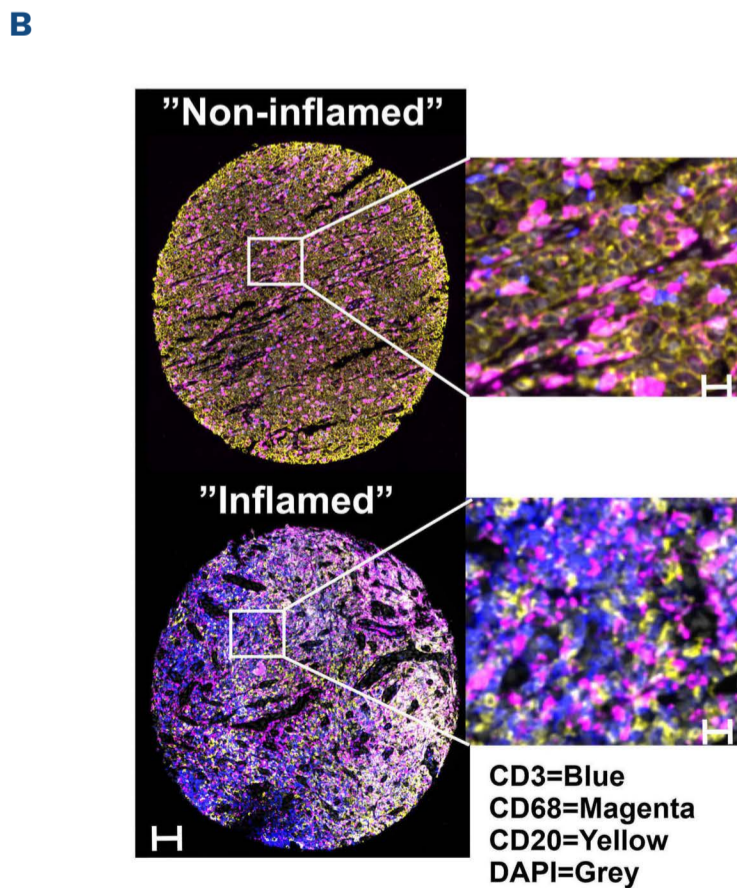
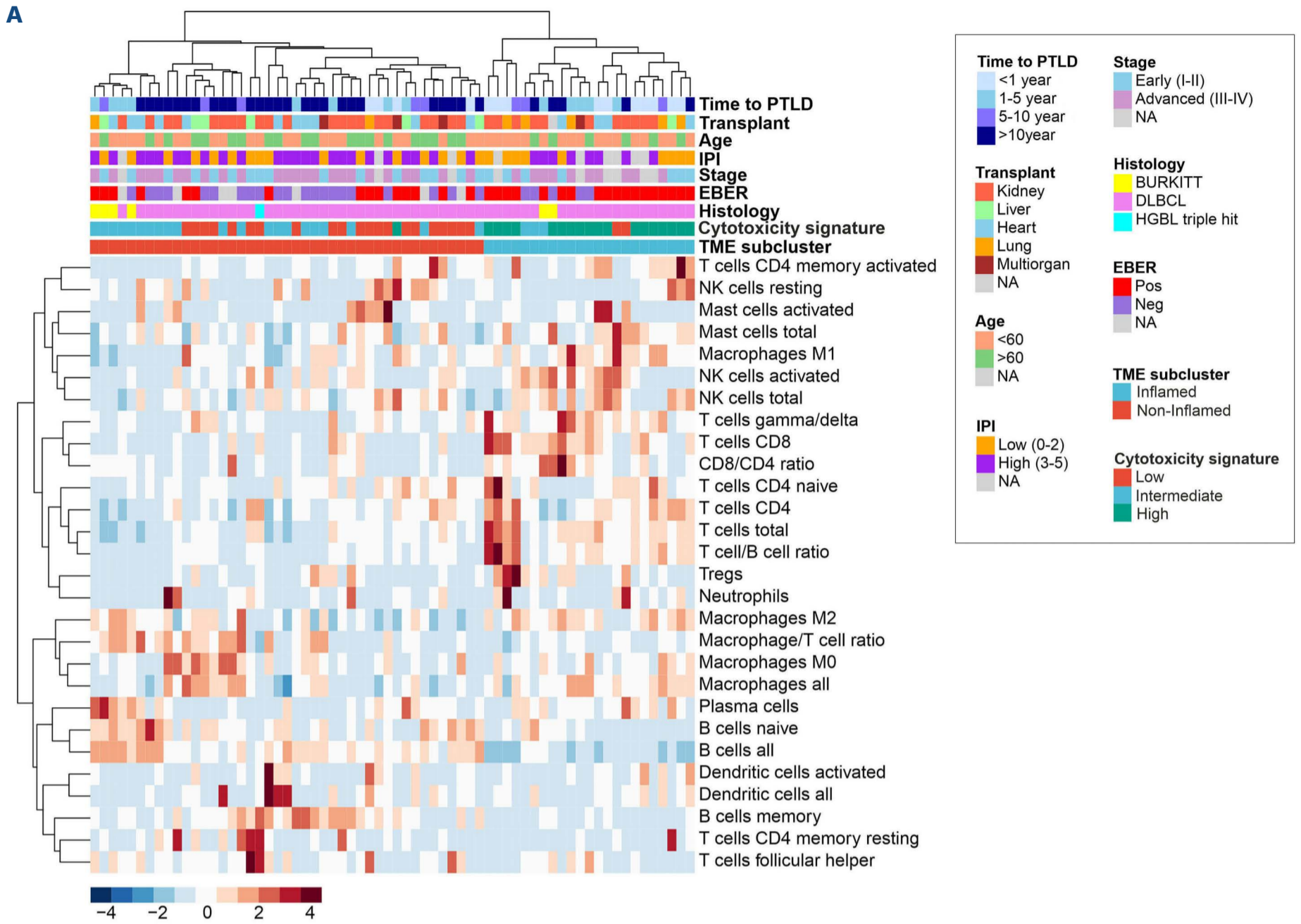


**Figure 3. Cytotoxicity gene signature predicts better outcome in post-transplant aggressive B-cell lymphoma.** (A) Heatmap showing the unsupervised hierarchical clustering of genes associated with cytotoxicity. (B, C) Kaplan-Meier plots with the overall survival (OS) (B) and progression-free survival (PFS). (C) Estimates of high, intermediate, and low expression of the cytotoxic signature. HR: hazard ratio. NA: not assigned; IPI: International Prognostic Index; EBER: Epstein-Barr virus-encoded small RNA; pos: positive; neg: negative; HGBL: high-grade B-cell lymphoma; DLBCL: diffuse large B-cell lymphoma.



Continued on following page.



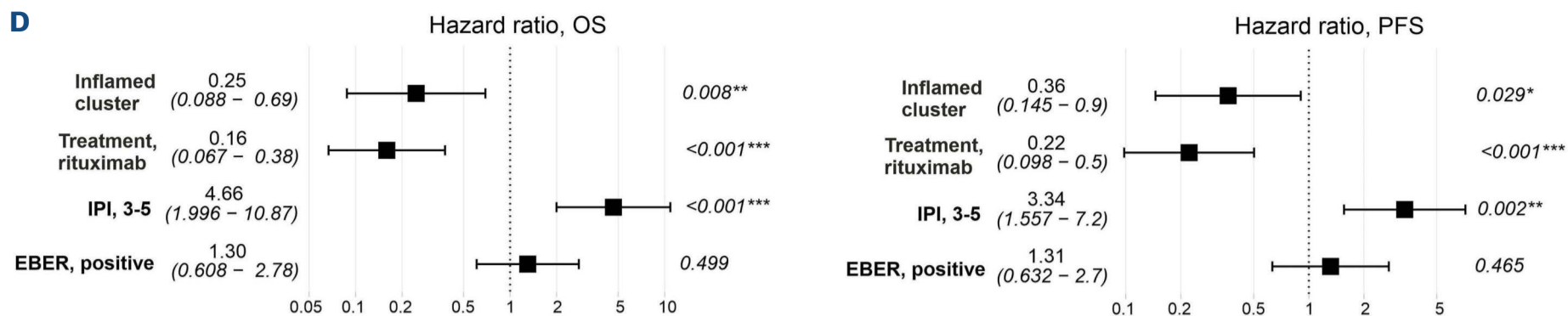


**Figure 4. Inflamed tumor microenvironment is associated with better survival in post-transplant aggressive B-cell lymphoma.**

(A) Heatmap visualizing the clustering of CIBERSORTx deconvoluted immune cell types. (B) Representative multiplex immunohistochemistry (mIHC) images of patients with non-inflamed and inflamed tumor microenvironment (TME). The inlets show magnified regions from the TMA cores, as indicated by the rectangles. Scale bar 75  $\mu$ m in the images with the whole TMA cores, and 20  $\mu$ m in the inlets. (C) Kaplan-Meier overall survival (OS) and progression-free survival (PFS) estimates of the inflamed and non-inflamed TME subclusters. (D) Forest plots visualizing the Cox regression multivariable OS (left panel) and PFS (right panel) analysis of the inflamed TME subcluster with rituximab-containing treatment, International Prognostic Index (IPI) and the Epstein-Barr virus (EBV) status. NA: not assigned; EBV: Epstein-Barr virus-encoded small RNA; HGBL: high-grade B-cell lymphoma; DLBCL: diffuse large B-cell lymphoma; mo: months.

S8A). However, based on the first principal component, EBV-positive PT-DLBCL were more distinct from DLBCL compared with EBV-negative PT-DLBCL (*Online Supplementary Figure S8B*). Despite the similarities, a supervised analysis identified a gene signature, which could separate PT-DLBCL from sporadic DLBCL (*Figure 5B, C*). Genes having higher expression in sporadic DLBCL were enriched for T-cell signaling and T cell-related pathways (e.g., CD4, FOXP3, HLA genes), indicating that T-cell proportions are lower in PT-DLBCL (*Online Supplementary Table S5*). Indeed, this was verified by CIBERSORTx analysis, which confirmed that PT-DLBCL have lower proportions of T cells, in particular  $T_{FH}$  cells and  $\gamma\delta$  T cells, and resting mast cells (*Figure 5D; Online Supplementary Figure S8C*). In contrast, the proportions of NK cells, dendritic cells, plasma cells, and activated mast cells were higher in PT-DLBCL compared with sporadic DLBCL.

## Discussion

PTLD represent a heterogeneous spectrum of diseases ranging from early lesion and polymorphic lymphoproliferation to monomorphic lymphoma.<sup>2,3</sup> PTLT also comprise various histologic subtypes, of which DLBCL is the most common. In this study, we focused on profiling the TME of 75 PT-ABCL utilizing digital gene expression profiling complemented with *in silico* phenotyping of TME-associated immune cells. To our knowledge, this is one of the largest gene expression profiling studies so far conducted on PTLT. Recently, a multidimensional characterization of PTLT TME and virome presented distinct immunogenomic features reflecting divergent PTLT biology.<sup>28</sup> Here, we show that the PT-ABCL TME is heterogeneous and can be classified as inflamed and non-inflamed according to the proportions of distinct immune cells. Although the PT-

ABCL TME is affected by the immunosuppressive therapy, a subset of patients displayed higher expression of cytotoxicity gene signature and an inflamed TME rich in T cells, translating to improved survival. Interestingly, the patient subgroup with low cytotoxicity signature expressed higher levels of B-cell receptor associated genes (*PAX5, CD79A/B, CD19, MS4A1, SYK, BTK; data not shown*), allowing speculation that these patients could benefit from targeted therapies, such as CD79B-targeting polatumumab-vedotin,<sup>29-31</sup> CD19-targeting tafasitamab in combination with lenalidomide,<sup>32-34</sup> and SYK inhibitors.<sup>35,36</sup> The subgroup with the inflamed TME was enriched for EBV-positive cases, which is in accordance with previous findings suggesting that T cells react to the EBV antigens and are attracted to the site of the lymphoma.<sup>22</sup> In addition, EBV-positive and EBV-negative PTLT have been shown to form distinct entities with differences in the genomic and transcriptomic profiles.<sup>9,22,37</sup> However, in line with other studies,<sup>38-40</sup> EBV status itself was not prognostic in our cohort, suggesting that the favorable effect of the inflamed TME did not just reflect the EBV status. This was also supported by the multivariable analysis, which demonstrated that the inflamed TME was independent of IPI and EBV status in predicting favorable outcome.

We also compared TME between PT-DLBCL and sporadic DLBCL. Our data indicate that PT-DLBCL and sporadic DLBCL do not cluster into distinct subgroups based on the immune response gene expression or TME characteristics. In general, sporadic DLBCL had higher proportions of T cells, and their gene expression profile was enriched for T-cell-related genes. The lack of T cells in the PT-DLBCL was even more evident, when EBV-negative PT-DLBCL were compared with sporadic DLBCL. This represents the main difference between PT-DLBCL and sporadic DLBCL and associates with the immunosuppressive treatment of PTLT. In previous studies, EBV-

negative PT-DLBCL have been shown to resemble DLBCL genomically and transcriptionally, whereas EBV-positive PT-DLBCL have been considered more distinct; their transcriptomic profile substantially impacted by the EBV infection.<sup>8,9,22,37,41</sup> Unfortunately, EBV status of the sporadic DLBCL in our study was not available for comparison. Another limitation of our study is that it is based solely on gene expression profiling. Therefore, the association of TME on distinct genomic alterations could not be addressed. Considering that stromal signatures associate

with distinct genomic abnormalities and outcome in DLBCL,<sup>42-44</sup> it will be interesting to study the relationship between genomic abnormalities and microenvironmental signatures in PTLD as well.

In the solid organ setting, therapy of PTLD consists of reduction of immunosuppression and is often followed by CD20 antibody rituximab in combination with chemotherapy, such as CHOP (cyclophosphamide, doxorubicin, vincristine, and prednisone). However, since the PTLD patients are clinically fragile, intensive chemotherapy is not the pre-

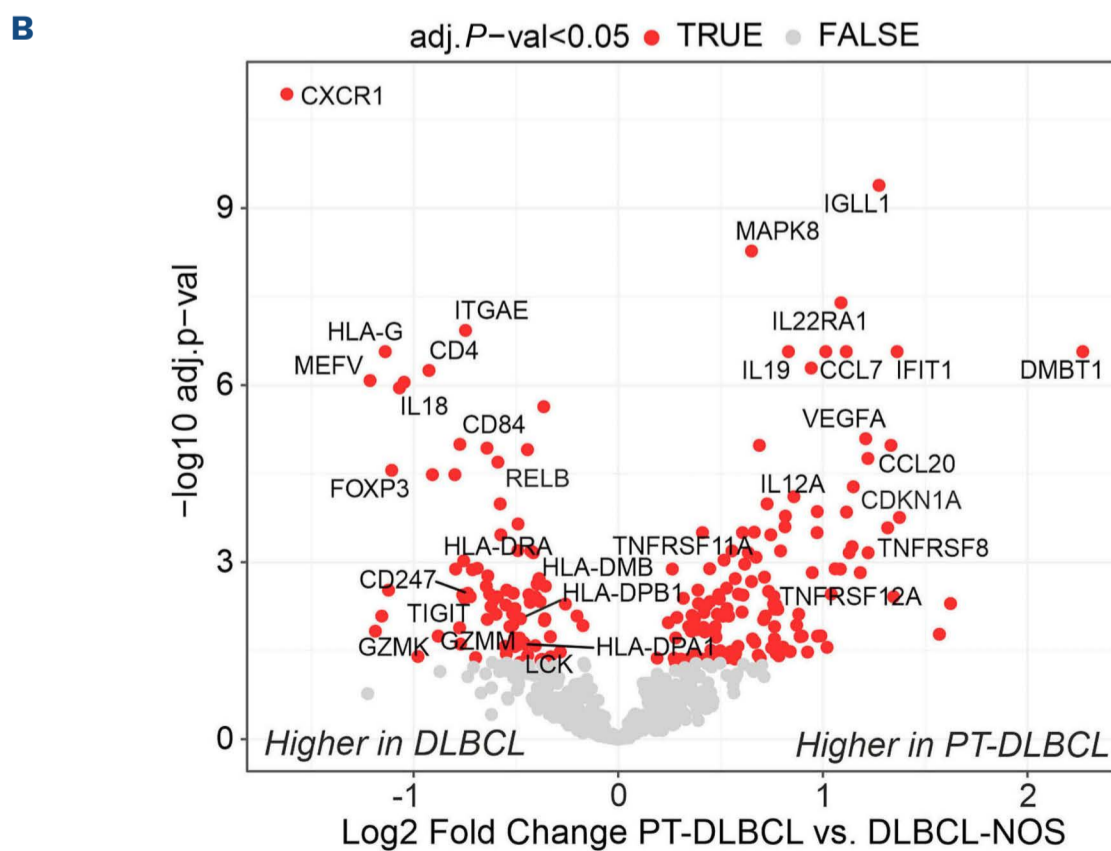
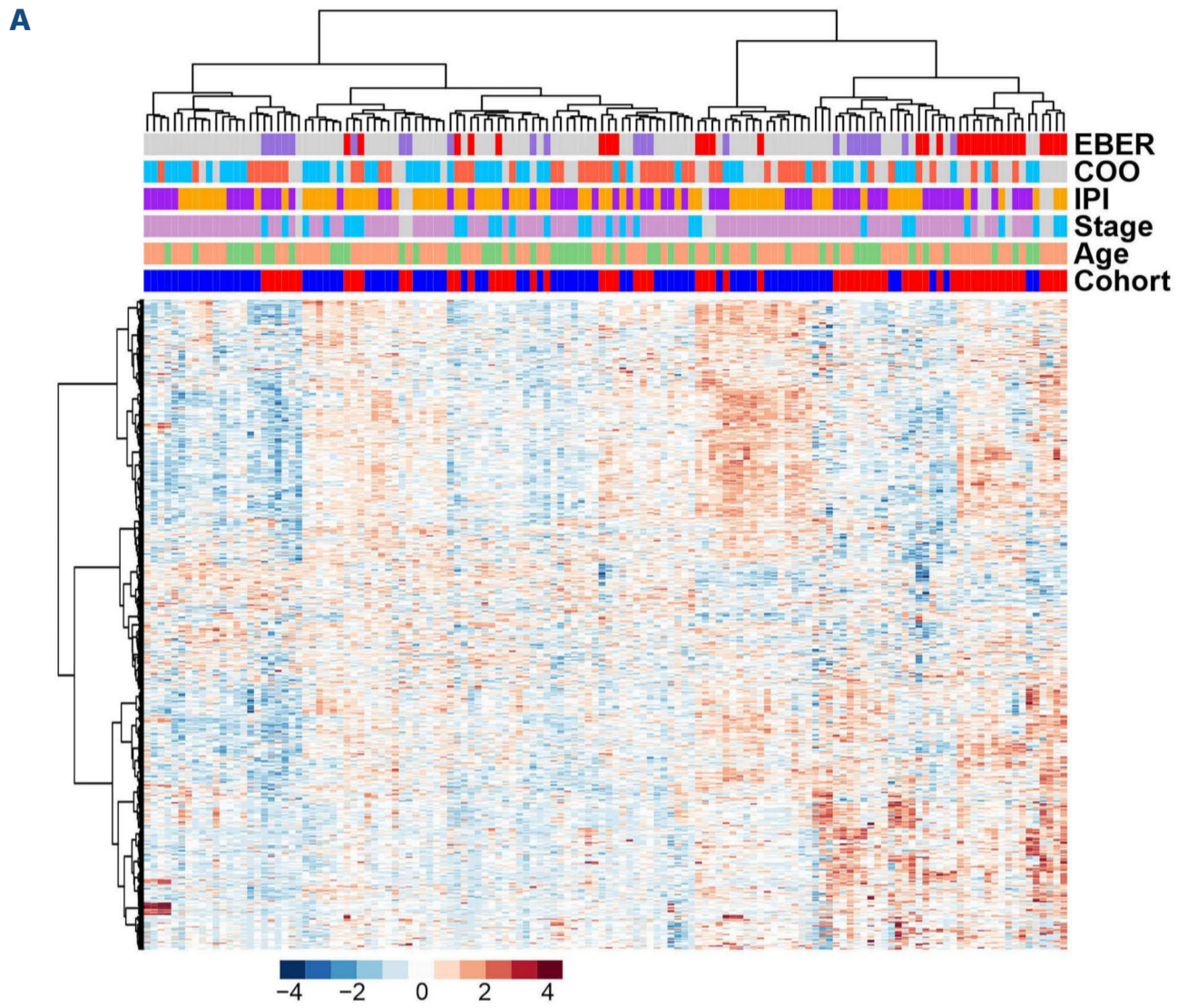
**Table 2.** Patient characteristics in the non-inflamed and inflamed groups.

Characteristics	Non-inflamed, N (%)	Inflamed, N (%)	P
Patients	43 (100)	23 (100)	
Age in years			0.122
<60	23 (53)	17 (74)	
≥60	20 (47)	6 (26)	
Stage			1.000
Early (1-2)	16 (4)	7 (30)	
Advanced (3-4)	24 (56)	10 (43)	
NA	3 (7)	6 (26)	
IPI			0.397
Low (0-2)	16 (37)	9 (39)	
High (3-5)	24 (56)	8 (35)	
NA	3 (7)	6 (26)	
EBER			0.008
Negative	21 (49)	5 (22)	
Positive	15 (35)	18 (78)	
NA	7 (16)	0	
Histology			1.000
DLBCL	38 (89)	21 (92)	
Burkitt	4 (9)	2 (8)	
HGBL triple hit	1 (2)	0	
Time from transplant in years to PTLD			0.004
<1	4 (9)	10 (43)	
1-5	8 (19)	5 (22)	
5-9	5 (12)	3 (13)	
≥10	26 (60)	5 (22)	
Transplant			0.169
Kidney	21 (49)	11 (48)	
Heart	11 (25)	4 (17)	
Liver	6 (14)	1 (4)	
Lung	2 (5)	5 (22)	
Multiorgan	3 (7)	1 (4)	
NA	0	1 (4)	
Rituximab-containing treatment			1.000
No	9 (21)	5 (22)	
Yes	33 (77)	18 (78)	
NA	1 (2)	0	
Treatment response			0.082
CR	22 (51)	18 (78)	
PR	4 (9)	0	
SD	2 (5)	2 (9)	
PD	6 (14)	0	
NA	9 (21)	3 (13)	

NA: not assigned; IPI: International Prognostic Index; EBER: Epstein Barr-virus-encoded small RNA; DLBCL: diffuse large B-cell lymphoma; HGBL: high-grade B-cell lymphoma; PTLD: post-transplant lymphoproliferative disorder; CR: complete response; PR: partial response; SD: stable disease; PD: progressive disease.

ferred choice in the first-line therapy.<sup>45</sup> In our cohort, the majority (71%) of the patients were treated with a rituximab-containing regimen, and over half of the patients also received chemotherapy. A limitation of our study was that information about the type of immunosuppressive therapy

used in the PTLD patients was not available for the analyzes. Immunosuppressive therapy can have a significant impact on the TME in PTLD by reducing the number and function of immune cells within the TME and thus leading to a less favorable TME, which promotes lymphoma growth



Continued on following page.

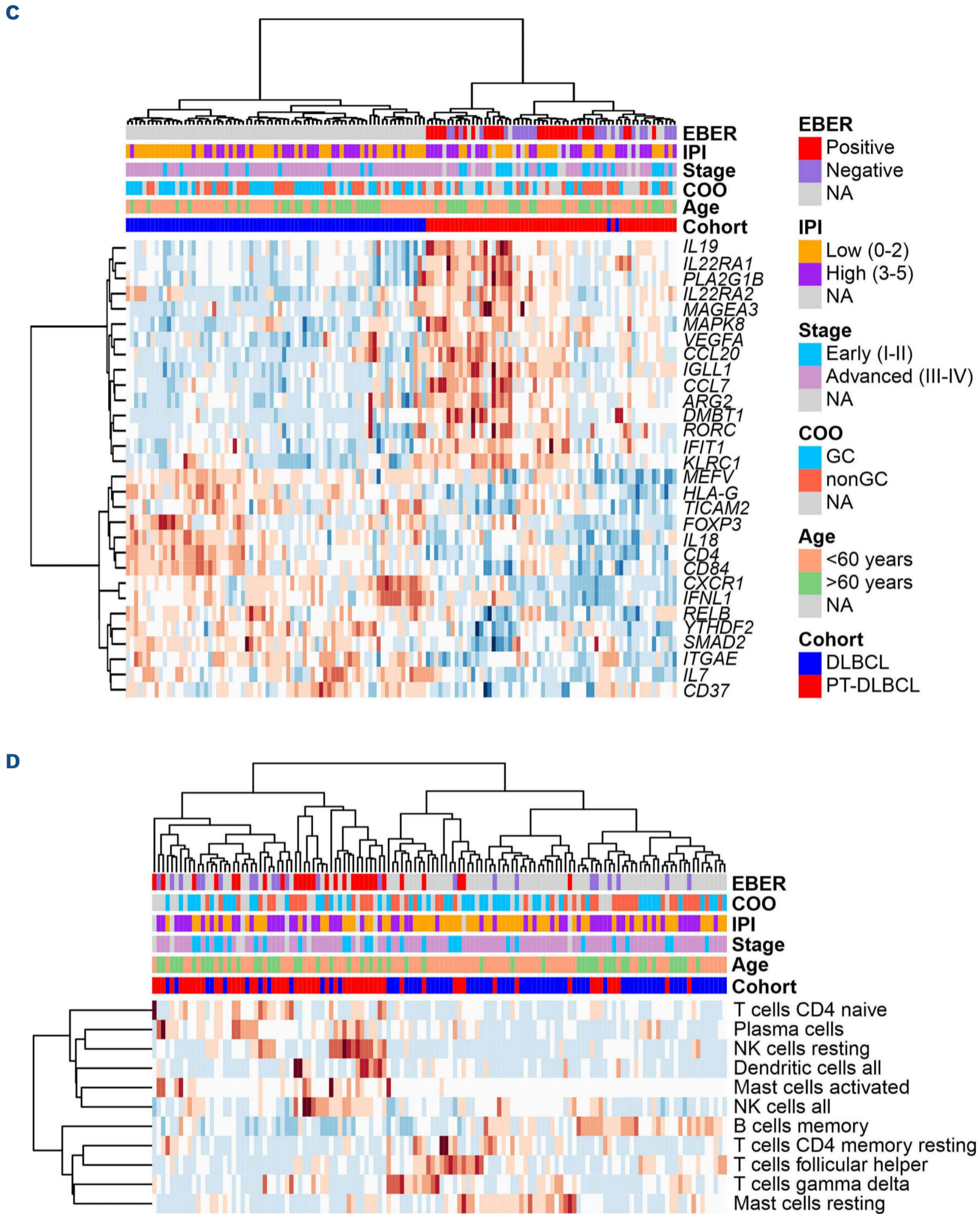


**Figure 5. Comparison of post-transplant diffuse large B-cell lymphoma with immunocompetent host diffuse large B-cell lymphoma.** (A) Heatmap illustrating unsupervised hierarchical clustering of the immune panel gene expression in post-transplant lymphoproliferative disorder (PTLD) with diffuse large B-cell lymphoma (DLBCL) histology (N=59) and DLBCL from immunocompetent patients (N=75). (B) Volcano plot showing differentially expressed genes in post-transplant DLBCL (PT-DLBCL) compared to DLBCL. Genes denoted in red are significantly (adj.  $P < 0.05$ ) differentially expressed. Selected genes are annotated in the plot. (C) The heatmap visualizes clustering of PT-DLBCL and DLBCL based on the expression of the most significant (adj.  $P < 0.0001$ ) differentially expressed genes. (D) Immune cell proportions were deconvoluted by CIBERSORTx. Cell types that have differential levels in PT-DLBCL compared to DLBCL ( $P < 0.05$ ) are visualized in the heatmap. NA: not assigned; IPI: International Prognostic Index; EBER: Epstein-Barr virus-encoded small RNA; HGBL: high-grade B-cell lymphoma; NK: natural killer; GC: germinal center; NOS: not otherwise specified; COO: cell of origin.

and progression.<sup>12</sup> In addition to its direct effects on immune cells, immunosuppressive therapy can impact the TME through its effects on the expression of cytokines and chemokines, such as interleukin-10 and interferon- $\gamma$ , which play a critical role in regulating immune cell functions. In general, heart, lung, intestinal, and multi-organ transplant recipients are attributed to more aggressive immunosuppression due to severe consequences of graft failure owing to the rejection.<sup>46</sup> In our study, the type of the transplant organ was, however, neither associated with the inflammation status of the PT-ABCL nor with the proportions of the distinct immune cells.

In conclusion, we provide a comprehensive phenotypic characterization of PT-ABCL that highlights the importance of TME biology and in particular T-cell infiltration, in the clinical behavior and prognosis of PTLT.

### Disclosures

SL consults for Genmab, Gilead, Incyte, Novartis, Roche, Abbvie and Orion; she has received research funding from Genmab, Nordic Nanovector, Novartis, Roche, Bayer and Celgene Hutchmed all outside of the submitted work; she has received honoraria from Novartis and Gilead. Other authors have no conflicts of interest to declare.

### Contributions

S-KL designed and conceived the study, analyzed data, and

wrote the manuscript. TF designed the study, collected clinical data, and contributed to writing the manuscript. MA analysed mIHC data. SV, AWJ, FA, S-JH-D, HH, KB, and PEK collected samples and provided clinical data. RR designed the study and revised the manuscript. SL designed and supervised the study and revised the manuscript. All authors have read and accepted the final version of the manuscript.

### Acknowledgements

We thank the DNA Sequencing and Genomics Laboratory at the Institute of Biotechnology, University of Helsinki for the NanoString analyzes, Anne Aarnio for technical assistance, and Annabrita Schoonenberg, Teijo Pellinen and FIMM Digital Microscopy and Molecular Pathology Unit supported by Hi-LIFE and Biocenter Finland for the mIHC services.

### Funding

This research was funded by the grants from the Academy of Finland (to SL), Finnish Cancer Organizations (to SL), Sigrid Juselius Foundation (to SL), University of Helsinki (to SL), Helsinki University Hospital (to SL) and ScandiTransplant (to TF).

### Data-sharing statement

The datasets generated during and/or analyzed during the current study are available from the corresponding author on reasonable request.

## References

1. Friman TK, Jaamaa-Holmberg S, Aberg F, et al. Cancer risk and mortality after solid organ transplantation: a population-based 30-year cohort study in Finland. *Int J Cancer*. 2022;150(11):1779-1791.
2. Alaggio R, Amador C, Anagnostopoulos I, et al. The 5th edition of the World Health Organization Classification of Haematolymphoid Tumours: Lymphoid Neoplasms. *Leukemia*. 2022;36(7):1720-1748.
3. Campo E, Jaffe ES, Cook JR, et al. The International Consensus Classification of Mature Lymphoid Neoplasms: a report from the Clinical Advisory Committee. *Blood*. 2022;140(11):1229-1253.
4. Swerdlow SH, Campo E, Pileri SA, et al. The 2016 revision of the World Health Organization classification of lymphoid neoplasms. *Blood*. 2016;127(20):2375-2390.
5. Crombie JL, LaCasce AS. Epstein Barr virus associated B-cell lymphomas and Iatrogenic lymphoproliferative disorders. *Front Oncol*. 2019;9:109.
6. Dierickx D, Tousseyn T, Gheysens O. How I treat posttransplant lymphoproliferative disorders. *Blood*. 2015;126(20):2274-2283.
7. Dierickx D, Habermann TM. Post-transplantation lymphoproliferative disorders in adults. *N Engl J Med*. 2018;378(6):549-562.
8. Ferla V, Rossi FG, Goldaniga MC, Baldini L. Biological difference between Epstein-Barr virus positive and negative post-transplant lymphoproliferative disorders and their clinical impact. *Front Oncol*. 2020;10:506.
9. Morscio J, Dierickx D, Ferreira JF, et al. Gene expression profiling reveals clear differences between EBV-positive and EBV-negative posttransplant lymphoproliferative disorders. *Am J Transplant*. 2013;13(5):1305-1316.
10. Craig FE, Johnson LR, Harvey SA, et al. Gene expression profiling of Epstein-Barr virus-positive and -negative monomorphic B-cell posttransplant lymphoproliferative disorders. *Diagn Mol Pathol*. 2007;16(3):158-168.
11. Scott DW, Gascoyne RD. The tumour microenvironment in B cell lymphomas. *Nat Rev Cancer*. 2014;14(8):517-534.
12. Marcelis L, Tousseyn T. The tumor microenvironment in post-transplant lymphoproliferative disorders. *Cancer Microenviron*. 2019;12(1):3-16.
13. Holte H, Leppa S, Bjorkholm M, et al. Dose-densified chemoimmunotherapy followed by systemic central nervous system prophylaxis for younger high-risk diffuse large B-cell/follicular grade 3 lymphoma patients: results of a phase II Nordic Lymphoma Group study. *Ann Oncol*. 2013;24(5):1385-1392.
14. Leppa S, Jorgensen J, Tierens A, et al. Patients with high-risk DLBCL benefit from dose-dense immunochemotherapy combined with early systemic CNS prophylaxis. *Blood Adv*. 2020;4(9):1906-1915.
15. Autio M, Leivonen SK, Bruck O, et al. Immune cell constitution in the tumor microenvironment predicts the outcome in diffuse large B-cell lymphoma. *Haematologica*. 2021;106(3):718-729.
16. Newman AM, Liu CL, Green MR, et al. Robust enumeration of cell subsets from tissue expression profiles. *Nat Methods*. 2015;12(5):453-457.
17. Newman AM, Steen CB, Liu CL, et al. Determining cell type

- abundance and expression from bulk tissues with digital cytometry. *Nat Biotechnol.* 2019;37(7):773-782.
18. Dave SS, Fu K, Wright GW, et al. Molecular diagnosis of Burkitt's lymphoma. *N Engl J Med.* 2006;354(23):2431-2442.
  19. Montesinos-Rongen M, Brunn A, Bentink S, et al. Gene expression profiling suggests primary central nervous system lymphomas to be derived from a late germinal center B cell. *Leukemia.* 2008;22(2):400-405.
  20. Grommes C, DeAngelis LM. Primary CNS lymphoma. *J Clin Oncol.* 2017;35(21):2410-2418.
  21. Bollard CM, Rooney CM, Heslop HE. T-cell therapy in the treatment of post-transplant lymphoproliferative disease. *Nat Rev Clin Oncol.* 2012;9(9):510-519.
  22. Morscio J, Finalet Ferreira J, Vander Borgh S, et al. Identification of distinct subgroups of EBV-positive post-transplant diffuse large B-cell lymphoma. *Mod Pathol.* 2017;30(3):370-381.
  23. Ansell SM, Stenson M, Habermann TM, Jelinek DF, Witzig TE. Cd4+ T-cell immune response to large B-cell non-Hodgkin's lymphoma predicts patient outcome. *J Clin Oncol.* 2001;19(3):720-726.
  24. Keane C, Gill D, Vari F, Cross D, Griffiths L, Gandhi M. CD4(+) tumor infiltrating lymphocytes are prognostic and independent of R-IP1 in patients with DLBCL receiving R-CHOP chemotherapy. *Am J Hematol.* 2013;88(4):273-276.
  25. Keane C, Vari F, Hertzberg M, et al. Ratios of T-cell immune effectors and checkpoint molecules as prognostic biomarkers in diffuse large B-cell lymphoma: a population-based study. *Lancet Haematol.* 2015;2(10):e445-455.
  26. Autio M, Leivonen SK, Bruck O, Karjalainen-Lindsberg ML, Pellinen T, Leppa S. Clinical impact of immune cells and their spatial interactions in diffuse large B-cell lymphoma microenvironment. *Clin Cancer Res.* 2022;28(4):781-792.
  27. Leivonen SK, Pollari M, Bruck O, et al. T-cell inflamed tumor microenvironment predicts favorable prognosis in primary testicular lymphoma. *Haematologica.* 2019;104(2):338-346.
  28. Schroers-Martin J, Garofalo A, Soo J, et al. Tumor microenvironment determinants of immunotherapy response identified by integrated host & viral analysis of post-transplant lymphoproliferative disorders. *Blood.* 2022;140(Suppl 1):S172-174.
  29. Sehn LH, Hertzberg M, Opat S, et al. Polatuzumab vedotin plus bendamustine and rituximab in relapsed/refractory DLBCL: survival update and new extension cohort data. *Blood Adv.* 2022;6(2):533-543.
  30. Tilly H, Morschhauser F, Sehn LH, et al. Polatuzumab vedotin in previously untreated diffuse large B-cell lymphoma. *N Engl J Med.* 2022;386(4):351-363.
  31. Sehn LH, Herrera AF, Flowers CR, et al. Polatuzumab vedotin in relapsed or refractory diffuse large B-cell lymphoma. *J Clin Oncol.* 2020;38(2):155-165.
  32. Delgado J, Papadouli I, Sarac SB, et al. The European Medicines Agency review of tafasitamab in combination with lenalidomide for the treatment of adult patients with relapsed/refractory diffuse large B-cell lymphoma. *Hemasphere.* 2021;5(12):e666.
  33. Nowakowski GS, Yoon DH, Peters A, et al. Improved efficacy of tafasitamab plus lenalidomide versus systemic therapies for relapsed/refractory DLBCL: RE-MIND2, an observational retrospective matched cohort study. *Clin Cancer Res.* 2022;28(18):4003-4017.
  34. Salles G, Duell J, Gonzalez Barca E, et al. Tafasitamab plus lenalidomide in relapsed or refractory diffuse large B-cell lymphoma (L-MIND): a multicentre, prospective, single-arm, phase 2 study. *Lancet Oncol.* 2020;21(7):978-988.
  35. Friedberg JW, Sharman J, Sweetenham J, et al. Inhibition of Syk with fostamatinib disodium has significant clinical activity in non-Hodgkin lymphoma and chronic lymphocytic leukemia. *Blood.* 2010;115(13):2578-2585.
  36. Flinn IW, Bartlett NL, Blum KA, et al. A phase II trial to evaluate the efficacy of fostamatinib in patients with relapsed or refractory diffuse large B-cell lymphoma (DLBCL). *Eur J Cancer.* 2016;54:11-17.
  37. Ferreira JF, Morscio J, Dierickx D, et al. EBV-positive and EBV-negative posttransplant diffuse large B cell lymphomas have distinct genomic and transcriptomic features. *Am J Transplant.* 2016;16(2):414-425.
  38. Luskin MR, Heil DS, Tan KS, et al. The impact of EBV status on characteristics and outcomes of posttransplantation lymphoproliferative disorder. *Am J Transplant.* 2015;15(10):2665-2673.
  39. Evens AM, David KA, Helenowski I, et al. Multicenter analysis of 80 solid organ transplantation recipients with post-transplantation lymphoproliferative disease: outcomes and prognostic factors in the modern era. *J Clin Oncol.* 2010;28(6):1038-1046.
  40. Ghobrial IM, Habermann TM, Maurer MJ, et al. Prognostic analysis for survival in adult solid organ transplant recipients with post-transplantation lymphoproliferative disorders. *J Clin Oncol.* 2005;23(30):7574-7582.
  41. Menter T, Juskevicius D, Alikian M, et al. Mutational landscape of B-cell post-transplant lymphoproliferative disorders. *Br J Haematol.* 2017;178(1):48-56.
  42. Kotlov N, Bagaev A, Revuelta MV, et al. Clinical and biological subtypes of B-cell lymphoma revealed by microenvironmental signatures. *Cancer Discov.* 2021;11(6):1468-1489.
  43. Lenz G, Wright G, Dave SS, et al. Stromal gene signatures in large-B-cell lymphomas. *N Engl J Med.* 2008;359(22):2313-2323.
  44. Monti S, Savage KJ, Kutok JL, et al. Molecular profiling of diffuse large B-cell lymphoma identifies robust subtypes including one characterized by host inflammatory response. *Blood.* 2005;105(5):1851-1861.
  45. Trappe RU, Dierickx D, Zimmermann H, et al. Response to rituximab induction is a predictive marker in B-cell post-transplant lymphoproliferative disorder and allows successful stratification into rituximab or R-CHOP consolidation in an international, prospective, multicenter phase II trial. *J Clin Oncol.* 2017;35(5):536-543.
  46. Opelz G, Dohler B. Lymphomas after solid organ transplantation: a collaborative transplant study report. *Am J Transplant.* 2004;4(2):222-230.